

A Neural Optimization Framework for Zoom Lens Camera Calibration*

Moumen T. Ahmed

CVIP Lab. ECE Dept.
University of Louisville
Louisville, KY 40292
moumen@cvip.uofl.edu

Aly A. Farag

CVIP Lab. ECE Dept.
University of Louisville
Louisville, KY 40292
farag@cvip.uofl.edu

Abstract

Camera systems with zoom lenses are inherently more useful than those with passive lenses due to their flexibility and controllability. However, calibration techniques for active-cameras, still, lag behind those developed for calibration of passive-lens cameras. In this paper, we present a neural framework for zoom-lens camera calibration based on our proposed neuro-calibration approach, which maps the classical problem of geometric camera calibration into a learning problem of a multi-layered feedforward neural network (MLFN). After discussing the features and advantages of the neurocalibration network, we present how this neural framework can capture the complex variations in the camera model parameters, both intrinsic and extrinsic, while minimizing the calibration error over all the calibration data across continuous ranges in the lens control space. The framework consists of a number of MLFNs learning concurrently, independently and cooperatively, the perspective projection transformation of the camera over its optical setting ranges. The calibration results of this technique applied to Hitachi CCD cameras with H10x11E Fujinon active lenses are reported.

1 Introduction

Camera systems with zoom lenses are inherently more useful than those with fixed-parameter (*passive*) lenses due to their flexibility and controllability. In such *active* cameras, the optical parameters, i.e., zoom, focus and aperture are usually (computer) motor controlled. The capability of varying these parameters has found many important practical applications, e.g, for depth reconstruction [5], active vision [6] and active stereo reconstruction [15]. However, active lenses are not commonly used in machine vision

because it is difficult to model the camera's image formation process for continuous ranges of lens settings. As a consequence, active-lens calibration techniques lag behind the state-of-the-art calibration of passive-lens cameras, which has a very rich literature. This also justifies why some researchers currently resort to self-calibration techniques [17].

In cameras with active-lenses, the image-formation process varies with the lens optical settings, thus many of the camera model parameters are non-linear functions of the lens settings. The calibration problem of these cameras relies on formulating functions that describe the relationships between the camera model parameters and the lens settings. As opposed to passive cameras, this raises several challenges. First, the dimensionality of calibration data is large. Of course, this leads to longer calibration time (which is of no particular concern in this category of off-line calibration techniques). A second challenge is the potential difficulty in taking measurements across a wide range of imaging conditions (e.g., defocus and magnification changes) that can occur over the range of zoom and focus control parameters.

The zoom-lens calibration approach, generally, involves first calibrating a conventional static camera model at a number of lens settings which span the lens control space using traditional calibration techniques. The calibrated model parameters (both intrinsic and extrinsic) at each lens setting can be stored in lookup tables and functional interpolation calculates values for intermediate lens settings (e.g., [4],[13]). An alternative approach is to model the parameter variations across continuous ranges of lens settings with functions fitted to the calibrated values [14],[10],[8]. In [16], a combination of the two approaches was proposed; some parameters were stored in lookup tables while functions were formulated for the others. Table I summarizes the lens controllable parameters for the mentioned references.

*This research was partially supported by grants from NSF (ECS 9505674) and The Department of Defense (USNV N00014-97-11076).

Table 1: Lens controllable optical parameters for some previous approaches.

Reference	Zoom	Focus
[4]	✓	✓
[13]	✓	✓
[14]	✓	×
[10]	✓	×
[8]	✓	✓
[16]	×	✓

In the widely cited work of Wilson [8], an active camera was calibrated across continuous ranges of focus and zoom. He estimates camera parameters by performing Tsai’s algorithm [2] independently on images taken at various settings of zoom and focus. Low order bivariate polynomials are fitted for some parameters (e.g., focal length, principal point coordinates), while the other parameters (e.g., rotation angles) are fixed. Global optimization over all the calibration data is carried out to optimize the coefficients of fitted polynomials.

The global optimization stage is important to take into consideration the interaction and the dependency between the model parameters [16]. This step represents an advantage of the function-fitting approach over using a lookup table for the calibration of an active camera over continuous control ranges. On the other hand, since the question about the optimal function type is often difficult to answer, and polynomials, in many cases, fail to follow the complex variations in the model parameters, it will be advantageous to use a neural network approach.

In a recent work [19], we have proposed the neurocalibration approach which cast the classical geometric (passive) camera calibration problem into a learning problem of a multi-layered feedforward neural network (MLFN). Due to the features and advantages of this approach, we propose, in this paper, to use it as an optimization framework for the more difficult task of zoom-lens camera calibration over continuous ranges of lens settings. We believe that a complete neural framework is well suited to this task, which can be looked at as a combination of passive camera calibration and function interpolation over a large collection of data. Therefore, if we add to the proven power of neural networks as universal approximators [11], the advantages of our neurocalibration technique, the combination will not only match our intuition, but will also provide a framework for global optimiza-

tion of the overall calibration error for the calibration data across continuous ranges of the lens control space. This framework consists of a number of MLFNs learning concurrently, independently and cooperatively, to capture the variations of model parameters across optical lens settings.

We describe the camera model and state the calibration problem in the next section. In Section 3, we briefly describe the neurocalibration approach and summarize its main features. An overview of the new framework for zoom-lens calibration is given in Section 4. Sections 5 and 6 describe our experiments and our concluding remarks.

2 Camera Calibration Problem

The result of camera calibration is an explicit transformation that maps a 3D world point $M = (X, Y, Z, 1)^\top$ into the 2D pixel $m = (u, v, 1)^\top$. In the pinhole model, the relationship between M and m is given by

$$s m = \mathbf{A}[\mathbf{R} \ \mathbf{t}] M \text{ with } \mathbf{A} = \begin{pmatrix} \alpha_u & c & u_0 \\ 0 & \alpha_v & v_0 \\ 0 & 0 & 1 \end{pmatrix}, \quad (1)$$

where s is an arbitrary scale factor; $(\mathbf{R} \ \mathbf{t})$, called the extrinsic parameters, are respectively the rotation (in terms of three angles: R_x, R_y and R_z) and translation ($\mathbf{t} = (t_x \ t_y \ t_z)^\top$) components of the camera transformation; \mathbf{A} is called the camera intrinsic matrix, and (u_0, v_0) are the coordinates of the principal point, α_u and α_v the scale factors in image u and v axes, and c the parameter describing the skewness of the two image axes. The camera mapping can be represented by a 3×4 projection matrix, \mathbf{P} , that encompasses all these parameters.

This camera model ignores lens distortion which is often accounted for in the camera model by adding some distortion parameters [2],[1]. However, these parameters can be estimated in the captured images by a pre-calibration process [7],[12]. Then all images can be undistorted before calibration proceeds. The decoupling between distortion parameters from the others will allow us to maintain the simple relation in (1) thus making following vision tasks (e.g., stereo reconstruction) easier. Moreover, the decoupling would minimize the effect of the correlation between lens distortion coefficients and other camera model parameters [3] on parameter estimation. The analysis and effects of this pre-calibration process are deferred to a follow-up work.

Given a sufficient number, N , of reference world

points, $M_i = (X_i \ Y_i \ Z_i \ 1)^\top$, as well as their corresponding pixel positions, $m_i = (u_i \ v_i \ 1)^\top$, the camera calibration problem is to estimate the 11 camera parameters, in other words, the projection matrix \mathbf{P} , that minimize

$$E = \sum_{i=1}^N \| \mathbf{P}M_i - m_i \|^2. \quad (2)$$

In Section 3, we give a summary of a MLFN that solves this problem. However, since the camera calibration parameters may vary as the lens setting is changed, the calibration problem of a zoom-lens camera system becomes finding the intrinsic and extrinsic camera parameters, expressed as functions of the controllable camera settings, which can be composed for any fixed camera setting in order to obtain the projection matrix. This problem is addressed in Section 4.

3 Neurocalibration

In [19] we proposed a MLFN that not only learns perspective projection mapping of a camera, but also can specify the calibration parameters. Here, we give a brief summary of our approach. The interested reader can refer to [19] for more details. The neurocalibration net has a topology of 4 – 4 – 3 with linear hidden and output neurons (see the central net in Fig. 1). The weight matrix of the hidden layer is denoted by \mathbf{V} , and it is assumed to correspond to the extrinsic parameters. The weight matrix of the output layer is denoted \mathbf{W} and it corresponds to the intrinsic parameters, or matrix \mathbf{A} . For any input pattern M_i , the network output, $(o_{ik}, k = 1, 2, 3)$, represents the 2D pixel homogeneous coordinates. In terms of the network parameters, the error in (2) can be expressed as [19]

$$E = \sum_{i=1}^N (\gamma_i o_{i1} - u_i)^2 + (\gamma_i o_{i2} - v_i)^2 + (\gamma_i o_{i3} - 1)^2, \quad (3)$$

where γ_i is a parameter attached to each input point, and takes care of the scale factor, s , in (1). One can look at γ_i as the slope of the linear activation function of the output neurons. The weights of the network W_{kj} and V_{ij} are initialized at random values in the range $-1 : 1$, while all the different γ_i are initially set to 1. The network weights W_{kj} , V_{ij} and γ_i are updated according to the gradient descent rule applied to Eq.(3) [19]. For ease of network learning, the input and desired patterns of the network are normalized by s_1 and s_2 , respectively. After training the network,

the projection matrix \mathbf{P} can be shown to be [19]

$$\mathbf{P} = \mathbf{S}_1 \mathbf{W} \mathbf{V} \mathbf{S}_2, \quad (4)$$

where

$$\mathbf{S}_1 = \text{diag}(s_1, s_1, 1) \text{ and } \mathbf{S}_2 = \text{diag}(s_2^{-1}, s_2^{-1}, s_2^{-1}, 1).$$

In order to go beyond just obtaining the matrix \mathbf{P} , the camera parameters are also obtained by mapping each network weight to one camera parameter. This can be done by enforcing the orthogonality constraints on \mathbf{R} during network learning. The constraints are represented as additional terms added to the error criterion to be minimized. The new error measure will be

$$E_{tot} = E_{2D} + \beta E_{orth}, \quad (5)$$

where E_{2D} is the same in (3) and E_{orth} is a sum of six error terms [19] that ensure the weights matrix \mathbf{V} to be a rotation matrix. The positive weighting factor, β , increases slowly as learning proceeds.

The network is trained by the traditional Backpropagation algorithm, however, speedup can be achieved by applying the conjugate gradient method during some periods of the training process. Switching between conjugate gradient and gradient descent can be done automatically (for details, see [9]).

Our extensive simulations and tests on practical images [19] yielded very low calibration error and have shown that this neurocalibration approach has the following features:

- it relaxes the requirement of a good initial starting point, which is common to other non-linear optimization techniques (e.g., Levenberg-Marquardt algorithm). These techniques often fail without this condition. In all the experiments conducted, the network has converged starting from random initial weights without sacrificing the calibration accuracy.
- experiments have shown very small sensitivity of the network learning to network parameters, e.g., learning constants.
- the orthogonality constraints on the rotation matrix are satisfied in the obtained parameters without extra optimization steps [1].
- it is simple; the reader can easily reproduce our code.
- it is interesting to note that the above network can be easily modified to calibrate some other

camera models [20], in particular, for calibrating linear pushbroom cameras [18] which may be thought of as a hybrid of perspective projection in one imaging direction and orthographic projection in the other direction.

These features motivated us to use the neurocalibration net for the global optimization step of zoom-lens calibration. In the techniques that use Levenberg-Marquardt algorithm (e.g., [14],[8]), if the initial values of the fitted parameters at the global optimization step are not adequate enough, no significant improvement in the calibration error is attained. In addition, if the optimization procedure takes no account of the structure of the orthonormal rotation matrix, the model rotation angles may end up with unpredictable values very far from the expected ranges.

4 Zoom-Lens Camera Calibration

In this section, we outline our framework for zoom lens calibration in the following three steps.

4.1 Passive Camera Calibration

The calibration process starts with collecting the calibration data; images of a calibration pattern are captured by the camera at a number of different lens optical settings (zoom, focus and/or aperture) covering the operating space of the camera. At each lens setting, the position of the calibration pattern in world coordinates is adjusted till a sharp focused image is obtained. The 3D coordinates of the pattern points are measured relative to a selected world coordinate system's origin using a 3D digitizer. The corresponding 2D pixels in each image are estimated with sub-pixel accuracy using a technique based on edge-detection and fitting [1],[2]. At each fixed lens setting, the fixed camera model parameters are estimated using the neurocalibration technique described in Section 3 (other calibration techniques may be used for this step).

4.2 Initial Parameter Formulation

Having obtained the parameters values at the different positions, we are ready to fit functions to these values. The skew, c , is fixed to zero. For ease of use of the camera model, excluding the translation component in the z-direction, the position and the orientation of the camera coordinate frame relative to the world coordinates are kept unchanged as the lens parameters are varied [8],[16]. Therefore, R_x , R_y , R_z , t_x and t_y are modeled with constants (zero-order terms). Constraining these parameters to be independent of optical settings makes use of the extra-degrees of freedom in the calibration (i.e., the dependency and correlation between some camera parameters for small

variations [16]). The initial values for the former five terms are set to their average values throughout the whole data. Then, for each of the remaining parameters, α_u , α_v , u_0 , v_0 , and t_z , a function is fitted across the optical settings using a MLFN. Each (from now on, *parameter*) MLFN has one output unit and in addition to the fixed bias, it has as many input units as the number of lens controllable parameters. The number of layers (two or more) and number of hidden units are determined experimentally for each MLFN alone. Note that these parameter MLFNs, unlike the neurocalibration network, have non-linear activation functions. Each MLFN is trained independently without the necessity of attaining a very low fitting error since this training is just an initial step before the global optimization step.

4.3 Global Optimization

The neurocalibration net has a central role in the global optimization step. It is trained using the Back-propagation algorithm to minimize the error in (5) over all the collected calibration data. The five zero-order terms are represented by five network weights, while the five parameter MLFNs serve to provide the central network with the rest of the weights representing the parameters that vary with the lens optical setting. Fig. 1 illustrates the central neurocalibration network and its associated MLFNs.

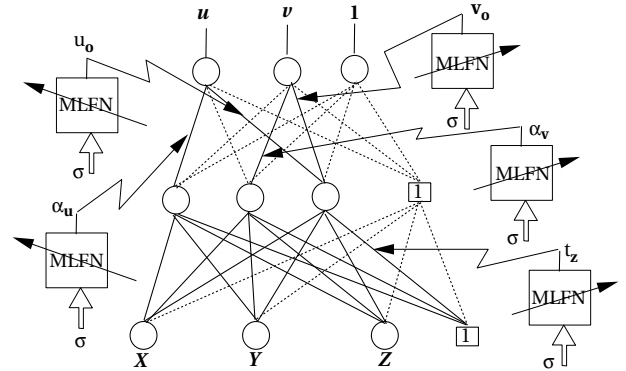


Figure 1: *Global optimization step: five parameter MLFNs cooperate with the central neurocalibration net during the optimization, σ denotes the lens controllable optical parameters and dashed links in the central network designate link weights fixed during learning at 0 or 1.*

At each lens setting, σ_i , the five parameter MLFNs provide the corresponding five model parameter values to the central network, which uses these values along

with the other zero-order term parameters to project all the input vectors, to compute the calibration error at this lens setting and to update all its weights. The five updated weights are propagated to the parameter MLFNs to update their functional mapping between the parameters and the lens settings. Note that each parameter MLFN minimizes its own fitting error, which is different from the calibration error computed by the central neurocalibration network. However, the fitting error of each parameter MLFN affects the calibration error. When the errors of all six networks drop below a small value, ϵ , each parameter MLFN has the final functional relationship of that particular parameter versus lens settings while the central network has the final values of the zero-order term parameters, namely R_x , R_y , R_z , t_x and t_y . Algorithm 1 shows an outline of the global optimization step.

Algorithm 1 Outline of global optimization step.

```

repeat
  CycleError = 0, Errork = 0, 1 ≤ k ≤ 5
  for all lens settings σi do
    parameter MLFNs supply 5 network weights.
    SettingError = 0.
    for all input-output patterns at σi do
      Compute calibration error, ε, from Eq.(5).
      All weights of central network are updated
      according to Backpropagation algorithm.
      SettingError += ε.
    end for
    CycleError += SettingError.
  Propagate the updated 5 network weights to
  corresponding MLFNs.
  Each parameter MLFN, k, updates its own
  Errork and performs, independently, a learning
  iteration according to Backpropagation algorithm.
end for
until CycleError < ε and Errork < ε, ∀k.

```

5 Experimental Results

In this section, we briefly describe the experiments conducted to calibrate two Hitachi HP-M1 CCD cameras with H10x11E Fujinon active lenses that are part of a trinocular active-vision system developed at our lab. The lens of these cameras has focal length 11mm - 110mm, focus range ∞ - 1.2m and iris range F1.9 - F22. The lens has 3 motors for iris, zoom and focus control. However, except for the iris motor, each of the other two motors provides a position reading presented as a dc voltage in the range 0 - 16384 after A/D conversion. In the following, we will refer to this range in

normalized presentation from 0 - 1. For the operating range, we have chosen a focus range of $0.5 \leq m_f < 1.0$ which corresponds roughly to a focused distance of 1.2m to 2.5m. For the zoom, we have chosen a similar range of $0.5 \leq m_z < 1.0$ which corresponds to focal length from approximately 11mm up to 25mm, while the iris is kept wide-open. We used a regular 7×7 sampling of the selected zoom and focus ranges. At each lens setting, an image was captured by the camera of a chessboard-like calibration pattern, thus a total of 49 sets of calibration data were obtained. Each set contained 440 data points. The calibration approach, explained in Section 4, was applied to the collected calibration data of each camera independently. In the global optimization stage, the networks were trained until the root mean square (*rms*) of calibration error dropped below 0.1 pixels, and the rms of fitting error for each parameter MLFN was below 0.1. Figure 2 illustrates some of the obtained parameter variations versus zoom and focus settings. For comparison sake,

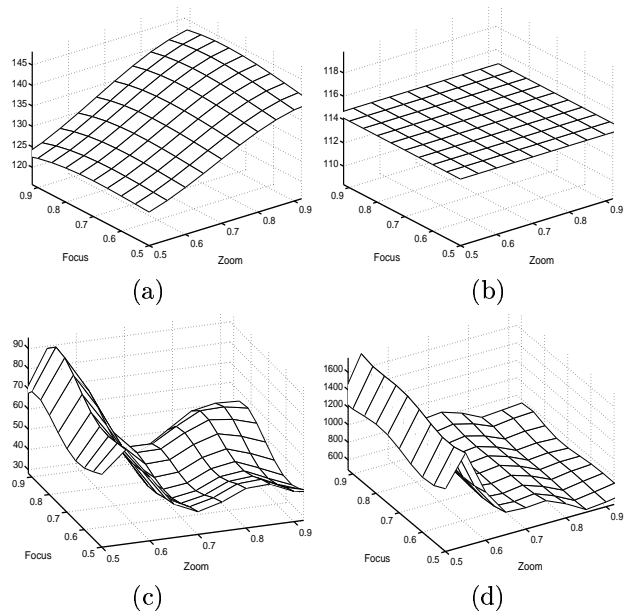


Figure 2: Variations of some model parameters versus normalized focus and zoom settings of one lens: (a) u_0 (pix.), (b) t_y (cm), (c) t_z (cm) and (d) α_u (pix.).

we applied Willson's approach [8] to the same collected calibration data (but using the camera model in Section 2 instead of Tsai's [2] that Willson used). Table II summarizes the order of bivariate polynomials selected for our implementation of Willson's approach and the MLFN topologies chosen to model the zoom and focus

varying parameters. Note that a bivariate polynomial of order q has $(q+1)(q+2)/2$ coefficients. In the global

Table 2: Polynomial orders and network topologies used to fit the zoom and focus varying parameters.

Parameter	poly. order	Net topology
t_z	5	2-5-1
u_0	3	2-3-1
v_0	3	2-3-1
α_u	6	2-5-2-1
α_v	6	2-5-2-1

optimization step using the Levenberg-Marquardt algorithm in Willson’s approach [8], the order of fitting the parameter polynomials to the data affects the final calibration error. Therefore, as Willson suggested, the polynomial coefficients of lowest order were optimized first followed by the higher ones in increasing order, using a greedy algorithm whenever two or more parameter models have the same polynomial order. The rms of calibration error in pixels is shown in Table III for the two cameras, computed over all 49×440 data points, before and after the global optimization step for the two methods. Since we have not imposed on

Table 3: Comparison of the rms of calibration error in pixels before and after global optimization between our proposed approach and Willson’s.

Approach	Camera 1		Camera 2	
	Init	Fin	Init	Fin
Willson’s	5.4	1.8	6.2	1.3
Ours	2.5	0.1	1.8	0.1

the calibration procedure the fact that the aspect ratio, α_v/α_u , should be nearly constant (from our earlier experience with these cameras, it is equal to 1) across the different lens settings, we used this to assess the results of our calibration. Our results, for both cameras, have shown a aspect ratio of 1 ± 0.05 across all zoom and focus calibrated ranges. Moreover, since the two cameras that we used form a stereo rig and we often captured images of the same calibration patterns by both of them, one can compute for these images the rms of the error in 3D reconstruction of the calibration pattern. This will serve as a quantitative measure of calibration accuracy. Table IV shows this measure computed, using 20 images, for the two approaches using the calibrated parameters before and

after the global optimization step. In fact, we have used this measure to validate the different parameter models and to circumvent over/under-fitting given the the size of the available data. Several experiments were necessary before we reached the previous models given in Table II. The calibration accuracy can be further improved if the images are corrected for lens distortion before calibration. Moreover, we can make use of more sampling positions (and thus more collected data size) to improve the accuracy.

Table 4: Rms of 3D reconstruction error in cm before and after global optimization.

Approach	Initial	Final
Willson’s	2.65	0.91
Ours	1.41	0.32

One can read from the above two tables the importance of the global optimization step to improve the calibration error. This step optimizes and refines the parameter-formulated functions taking into account the interaction and correlation between the different model parameters, which combine together to compose the camera projective transformation. This interaction is clearly absent in the function formulation step. The second thing to read from the tables is that our approach has been more able to capture the variations of the parameters across the lens settings. Rather than bivariate polynomials, other alternatives such as Chebyshev polynomials and Legendre polynomials could have been utilized. However, we resort to proven power of MLFNs [11] to provide a suitable parameter formulation. The last point that we like to emphasize is that even if MLFNs are used to provide this function mapping, the role of the neurocalibration network remains important to form an effective framework to optimize and refine these function mappings towards more accurate calibration results.

6 Summary and Conclusions

We have presented a new neural framework for zoom-lens camera calibration. The framework makes use of the neurocalibration network that maps the classical problem of geometric passive camera calibration into a learning problem of a MLFN. We summarized the features that this network has, which allow its usage as the heart of our active-camera calibration approach. The framework has three main steps: data collection and passive camera calibration, initial parameter formulation, and global optimization. In this

work, we stress the importance of the global optimization step to consider other factors missing in the initial parameter function-formulation step. Our experimental results have demonstrated better performance of our approach compared to Willson's approach, which is a reference of this domain. To improve the accuracy of our approach, more sampling positions during data collection need to be used along with removal of lens distortion [7],[12] from images before calibration. These two goals define our future directions in this work.

We believe that this approach has the following key features, as opposed to other techniques (e.g., [14],[10],[8],[16]):

1. it is general; it can consider, in a straightforward manner, any number/combination of lens control parameters, e.g., zoom, focus and/or aperture; since only the input layer of parameter MLFNs will be affected.
2. it can capture complex variations in the model parameters, both intrinsic and extrinsic, across control space.
3. all of the parameters are fitted to the calibration data at the same time, while in other approaches [14],[10],[8],[16], one parameter is fitted at a time and the final level of error generally depends on the order in which the models are fit to the data [8].

References

- [1] J. Weng, Paul Cohen and M. Herniou, "Camera calibration with distortion models and accuracy evaluation," *IEEE Trans. Patt. Anal. Machine Intell.*, Vol. 14, No. 10, Oct 1992.
- [2] Roger Tsai, "A versatile camera calibration technique for high-accuracy 3D machine vision metrology using off-the-shelf TV cameras and lenses," *IEEE Journal of Robotics and Automation*, Vol. RA-3, No. 4, Aug 1987.
- [3] S. Shih, Y. Hung and W. Lin, "Accuracy analysis on the estimation of camera parameters for active vision systems," *Proc. Int. Conf. Pattern Recognition (Vienna, Austria)*, Vol. 1, Aug 1996.
- [4] Mengxiang Li and Jean-Marc Lavest, "Some aspects of zoom lens camera calibration," *IEEE Trans. Patt. Anal. and Machine Intell.*, Vol. 18, Nov. 1996.
- [5] J. Lavest, G. Rives and M. Dhome, "3D reconstruction by zooming," *IEEE Trans. Robotics and Automation.*, Vol. 9, No. 2, April. 1993.
- [6] K. Pahlavan, T. Uhlin and J. Eklundh, "Active vision as a methodology", In *J. Aloimonos, editor, Active Perception, Lawrence-Erlbaum*, 1993.
- [7] R. Swaminathan and S. Nayar, "Non-metric calibration of wide-angle lenses and polycameras," *Proc. CVPR99, Fort Collins, Colorado*, June 1999.
- [8] R. G. Willson, "Modeling and calibration of automated zoom lenses", *PhD dissertation, Dept. Elect. Comp. Eng., Carnegie Mellon Univ.*, 1994.
- [9] T. Masters, "Advanced algorithms for neural networks: A C++ source book", *John Wiley*, 1995.
- [10] A. Wiley and K. Wong, "Geometric calibration of zoom lenses for computer vision metrology," *Photogrammetric Eng. Remote Sensing*, Vol. 61, No. 1, Jan. 1995.
- [11] F. Hornik, "Multilayer feedforward networks are universal approximators," *Neural Networks*, Vol. 2, 1989.
- [12] B. Prescott and G. McLean, "Line-based correction of radial lens distortion," *Graph. Models and Img. Process.*, Vol. 59, No. 1, Jan. 1997.
- [13] K. Tarabanis, R. Tsai and D. Goodman, "Calibration of a computer controlled robotic vision sensor with a zoom lens," *CVGIP: Image Understanding*, Vol. 59, No. 2, Jan. 1994.
- [14] W. Seales and D. Eggert, "Active-camera calibration using iterative image feature localization," *Proc. Int. Conf. Comp. Analysis of Images and Patterns, Prague*, Sept. 1995.
- [15] A. Abbott and N. Ahuja, "Active surface reconstruction by integrating focus, vergence, stereo, and camera calibration," *Proc. 3rd Int. Conf. Computer Vision.*, 1990.
- [16] S. Shih, Y. Hung and W. Lin, "Calibration of an active binocular head," *IEEE Trans. Man, Sys. and Cybernetics*, Vol. 28, No. 4, July 1998.
- [17] L. de Agapito, R. Hartley and E. Hayman "Linear self-calibration of a rotating and zooming camera," *Proc. Int. Conf. Computer Vision and Pattern Recognition, Fort Collins, CO*, Vol. 1, June 1999.
- [18] R. Gupta and R. Hartley, "Linear pushbroom cameras," *IEEE Trans. Patt. Anal. and Machine Intell.*, Vol. 19, No. 9, Sept. 1997.
- [19] M. Ahmed, E. Hemayed and A. Farag, "Neurocalibration: a neural network that can tell camera calibration parameters," *Proc. IEEE Int. Conf. Computer Vision, Korfu, Greece*, Sept. 1999.
- [20] M. Ahmed and A. Farag, "Calibration of Pushbroom cameras using neural networks," *Technical Report, CVIP Lab., Univ. of Louisville, KY*, Jan. 2000.